Proceeding of the IEEE
International Conference on Robotics and Biomimetics
Dali, China, December 2019

AFM Calibration of Nano-friction through Estimating Meniscus Water Membrane Contour between Single Polystyrene Nano-particle and Silicon Surface

Shuai Yuan, *Member, IEEE*, Tianshu Chu, Liyong Ma, Jing Hou, Junhai Wang

***Abstract*— In a certain humidity environment, the meniscus water membrane will greatly affect the nano-friction between the nano-particle and the substrate in the process of AFM nano-manipulation. Herein, a mathematical model for estimating the meniscus water membrane contour using infinitesimal iteration is employed, then near-spherical polystyrene nano-particles with radius from 50 nm to 300 nm were deposited on a silicon wafer for experiments using AFM after the tip is positioned and the friction between the nanoparticle and the substrate is measured. By analyzing the relationship between friction and effective contact area of water membrane and comparing with the existing work, the correctness and effectiveness of the method are proved.**

I. Introduction

AFM is a tool for characterization and manipulation at nano-scale by monitoring interaction between the tip and sample. Because of its high resolution [1], good repeatability and controllability, it has been widely used in nano-tribology. The pushing force of the nano-particle can be calculated through the force model during AFM nano-manipulation. In practice, environmental humidity is the key factor affecting nano-friction. Under a certain environmental humidity, the existence of the meniscus water membrane changes the nature of the interaction force between the nano-particle and the substrate, because the meniscus water membrane produces additional capillary force, which increases viscous adsorption between the nano-particle and the substrate. Capillary force is generally believed to be generated by a large negative Laplace pressure caused by surface tension in the meniscus water membrane[2]. This negative Laplace pressure adheres the particles together tightly with the substrate surface, forming a force called capillary pressure[3], which makes the viscous friction far greater than the coulomb friction caused by gravity[4]. Therefore, the capillary force becomes the main factor affecting the friction between the nano-particle and the substrate at nano-scale.

*Resrach supported by the National Natural Science Foundation of China (Project Codes: 61305125, 51805336), National Post Doctor Foundation (Project Codes: 2013M530955, 2014T70265)), and Liaoning Colleges and Universities Basic Scientific Research Project (LJZ2017046).

Shuai Yuan, is with Shenyang Jianzhu University, Shenyang, Liao Ning Province, China. Corresponding author to provide phone: +8610 13940077870; e-mail: reidyuan@163.com.

Tianshu Chu is with Shenyang Jianzhu University, Shenyang, Liao Ning Province, China. e-mail: 644095325@qq.com.

Liyong Ma was with Northeastern University, Liao Ning Province, China. e-mail: mly0817@126.com.

Jing Hou is with Shenyang Jianzhu University, Shenyang, Liao Ning Province, China. e-mail: 1015521052@qq.com.

Junhai Wang is with Shenyang Jianzhu University, Shenyang, Liao Ning Province, China. e-mail: jhwang@sjzu.edu.cn.

In order to explore the relationship between nano-friction and meniscus water membrane, it is necessary to calculate the contour of meniscus water membrane. Stanimir D.Iliev has proposed a dynamic contact angle estimation method based on Voinov hydrodynamic model, which can accurately get variation of the contact angle of water membrane contour during particle motion [5]. But it needs a lot of experiments and it is not suitable for nano-scale. Pakarinen O.H. and F.M. ORR also proposed methods for calculating the contour of water membrane in reference [6] and [7]. However, there is a lack of quantitative analysis of the influence of various factors on the contour such as contact angle, the distance between the substrate and the nano-particle.

We use AFM to measure the friction between the particle and the tip. During AFM tip motion, the non-linearity of PZT ($PbZrTiO_3$) and thermal drift of the system will result in uncertainties of tip positioning, which makes the position of the tip action point cannot be accurately controlled and leads to measurement errors of nano-friction. Therefore, it is necessary to localize the tip accurately during AFM nano-manipulation. Fig.1 shows that the AFM tip driven by the PZT has position uncertainties due to the PZT nonlinearity and the thermal drift. When using the traditional method for manipulating the nano-rod to connect the two electrodes, the tip uncertainties make it difficult to control the manipulation point on the nano-rod, which results in the nano-rod misalignment on the two electrode after manipulation. If the nano-particle is used as landmark for improving the tip position accuracy, the contact point can be controlled within the precision range for manipulating the nano rod to bridge the two electrodes.

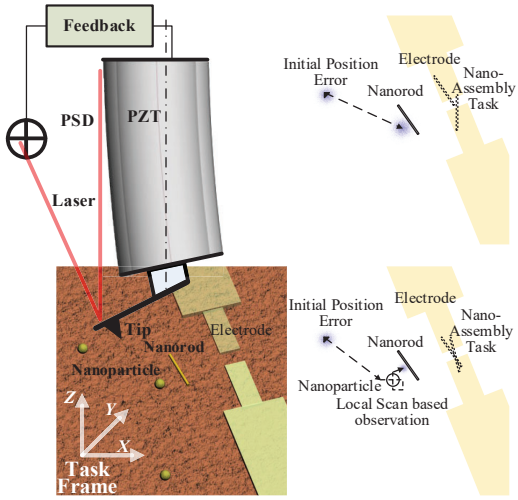

Fig.1 Effect of AFM tip uncertainties on nano-manipulation

978-1-7281-6321-5/19//$31.00 ©2019 IEEE

In this study, a mathematical model for estimating the meniscus water membrane contour using infinitesimal iteration is employed and the contour is calculated by simulation. Then landmark observation based tip position Estimation method is used to position the tip. After the tip is localized, the single polystyrene nano-particle is pushed in the vertical direction perpendicular to the cantilever for measuring the friction after the tip is positioned. Meanwhile, we compared the experimental result with the existing work to illustrate the correctness and effectiveness of this algorithm. Finally, the factors that may affect the effective contact area of water film are discussed.

II. Model of Water Membrane Contour

In order to obtain a general model, it is assumed that the particle is an axisymmetric sphere with a radius of less than 1000 nm. At this time, a certain size of water membrane can be formed between the nano-particle and the substrate, which makes a certain degree of humidity independence. Under these conditions, a coordinate system is established as shown in Fig.2 (b) [8]. Among them, the Z axis is the central axis of the nano-particle, Z_0 is the distance between the nano-particle and the substrate, r_1 is a negative vertical curvature radius of water membrane infinitesimal, r_2 is a positive curvature radius around the central axis, θ_1 is a contact angle between the starting point of water membrane and the particle surface, θ_2 is a contact angle between the end of water membrane and the substrate, α is an angle between the tangent of the starting point of the water membrane and the vertical line.

First, according to the Laplace-Yang equation[9], the radius of curvature at each point of the meniscus water membrane contour is:

$$r = 2(\frac{1}{r_1}+\frac{1}{r_2})^{-1} \tag{1}$$

The Kelvin radius is obtained from the Kelvin equation[10]:

$$r_k = \frac{\gamma \bullet v_0}{kT\ln(P^0 / P^{eq})} \tag{2}$$

Where, γ is the surface tension of gas-liquid interface, V_0 is the volume of liquid molecules, k is Boltzmann constant, T is the system temperature and P^0/P^{eq} is the relative humidity of the operating environment.

If the liquid condensation is in thermodynamic equilibrium with the surrounding water vapor, the mean radius of curvature at each point of the meniscus water membrane is approximately twice the Kelvin radius:

$$r = 2r_k$$

So the equation could be obtained:

$$r_k = (\frac{1}{r_1}+\frac{1}{r_2})^{-1} = \frac{\gamma \bullet v_0}{kT\ln(P^0 / P^{eq})} \tag{3}$$

In order to obtain water membrane contour, we use the method of infinitesimal iteration. First, an initial point on the particle surface is chosen as the starting point for contacting with the water membrane, and this point is used as the starting point of infinitesimal iteration. Since the infinitesimal length is small, it can be approximated as a continuous calculation. At the end of the infinitesimal, a segment perpendicular to the infinitesimal is made and it intersects with the central axis of the nano-particle, which is the positive curvature radius r_2 around the central axis, then r_1 can be obtained by equation (3). The selection of next infinitesimal needs to satisfy the curvature radius r_1 of the previous calculation, it means that the end of next infinitesimal is on the curvature circle of the vertical surface determined by the end of previous infinitesimal. The radius of curvature can be obtained from the formula of curvature radius:

$$r_1 = \frac{[1+(dx/dz)^2]^{3/2}}{d^2x/dz^2} \tag{4}$$

Since r_1 has been calculated, the direction of the next infinitesimal could be calculated:

$$d^2x = \frac{dz^2[1+(dx/dz)^2]^{3/2}}{r_1} \tag{5}$$

The infinitesimal is obtained by iterating calculation until the last infinitesimal intersects the substrate. If the angle between the last infinitesimal and the substrate satisfies the ideal termination angle, the contour of the water membrane will meet the requirement. Otherwise, the position of the initial infinitesimal will be reselected and the water membrane contour will be obtained iteratively until the termination angle is satisfied.

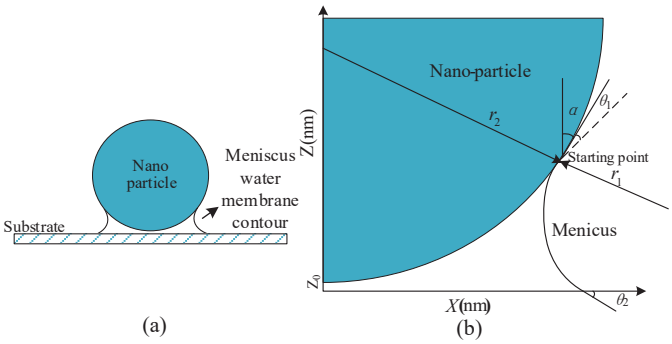

Fig.2 (a) Meniscus water membrane contour between nano-particle and substrate. (b) Mathematical model of water membrane contour

III. Simulation

A. Simulation system

We executed a numerical simulation in order to solve the meniscus water membrane contour. The solution of the water film is implemented in simulation. In the simulation, it is assumed that the starting angle of the water membrane is the same as the ending angle. According to the process of solving the water film contour model, we designed an algorithm program for solving the contour of the water film and the coordinates of the starting point. The flow chart is shown in the Fig.3.

In the program, we take the particle radius R, the starting point abscissa x_i, the r calculated by the Kelvin equation, the ordinate unit *DeltaY*, and the contact angle between the particle and the water film contour starting micro-element as input variables. The simulation result is a data point composed of an infinite number of micro-elements. These micro-elements are depicted in the figure, and are fitted to a

curve according to these position points, which is the water membrane contour.

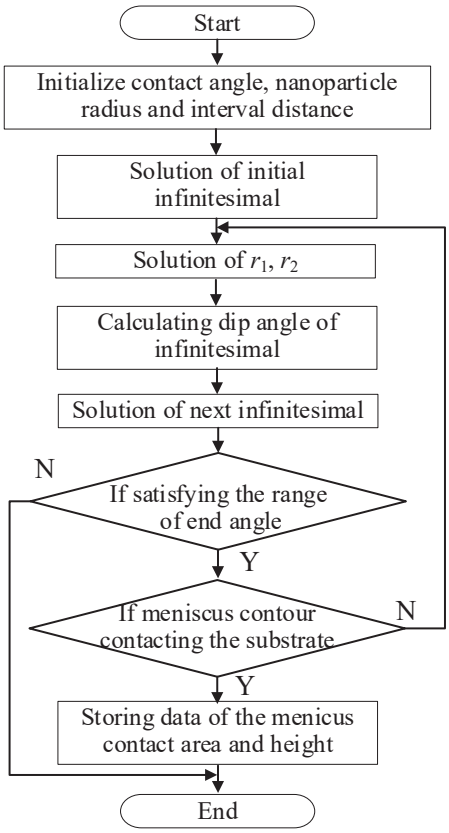

Fig.3 Flow chart of solving water membrane contour

B. Simulation result

In the simulation experiment, we used polystyrene nanoparticles with radiuses of 50 nm, 100 nm, and 300 nm for calculation. In the calculation, r=14 was calculated according to the experimental environment, *DeltaY* was 0.1, and the starting angle was 60°. The water film contours theoretically calculated by the simulation are shown in Fig.4, the radius of Figure 3(a)(b)(c) are 50,100,300 respectively.

IV. Experiment

A. Landmark Observation based Tip Position Estimation

AFM uses the tip as end effector for high-resolution observation and high-precision manipulation of the interesting region in task space. However, there is uncertainty in tip localization due to various factors. The tip position in task space is distributed in a region, and the region will gradually increase with movement of the tip. Therefore, it is difficult for observer to localize the tip precisely on the target when using AFM for nano-observation, and thus observer need to spend a lot of time adjusting their positions manually, which seriously hinders effective AFM nano-observation. AFM nano-manipulation is confronted with the same problem. It depends on the mechanical interaction between the tip and the manipulated object, so the precise position of the tip relative to the manipulated object is the prerequisite for successful manipulation. Because of the uncertainty of positioning tip in task space, it will seriously hinder the accurate localization of tip in the interesting region, which makes the most basic task of "moving from point A to point B" difficult to be achieved in robotics.

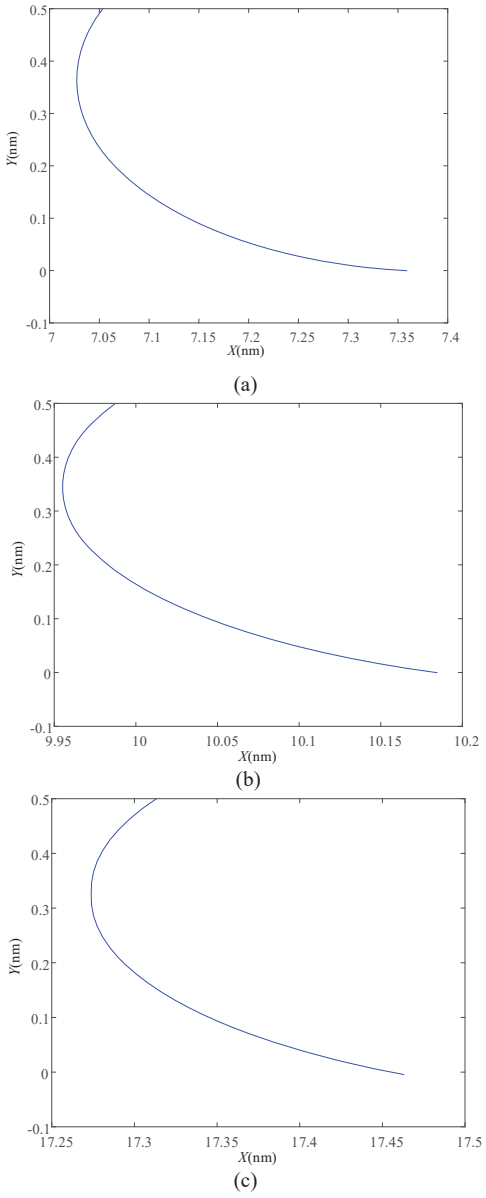

Fig.4 Simulation results

As for the system thermal drift and the PZT nonlinearity, SLAM method is used to reduce the tip position uncertainties [11]. As shown in Fig.5 (a), the features in the task space (nanoparticles) are used as landmarks to estimate the position of the tip by observing the relative distance between the tip and the landmark. When performing observations, the nanoparticles are scanned both horizontally and vertically (as shown in Fig.5 (b) to update the position of the tip. The position of the tip may drift because of the system thermal drift. As shown in Fig.5 (c), as for this problem, the tip needs

to observe the position of the center of the nanoparticle x_{kp} from the scan line of the current position x_k to the next position x_{k+1}. According to the position of x_{kp} in the task space, combined with the input control amount of the driving tip motion, the current position x_{k+i} of the tip can be estimated using Kalman filter.

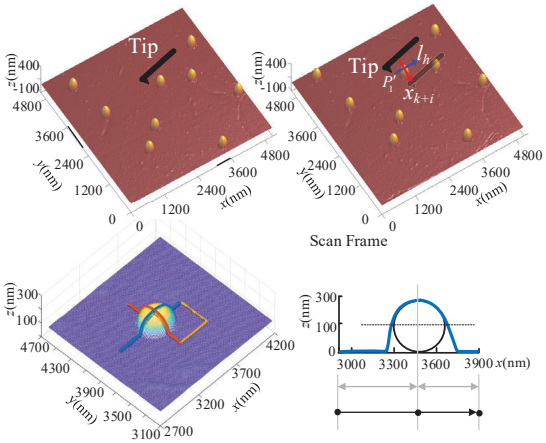

Fig.5 Positioning the tip through observing the nano-particle as the landmark.

B. Preparation for experiment

After the tip is positioned, we use polystyrene nano-particles produced by Poly Company with the radius of 50±1nm, 100±1nm, 300±1nm, which is of analytical purity. The polystyrene particles were chosen owing to their near-spherical shape, which will be a great deal easier for theoretical modeling. First, 100 mmol/l $MgCl_2$ solution is titrated on silicon wafer to increase friction. After drying, polystyrene particles are deposited respectively. In the experiment, Bruker ICON Atomic force microscope is used and the model of the tip is TESPA whose elastic modulus K_v is 42N/m.

C. Experimental results

The experimental data measured by AFM are shown in Fig.6, (a) is a schematic diagram of the AFM tip pushing the nanoparticles, (b) is the deflection of the cantilever in the horizontal and vertical directions respectively, and (c)(d)(e) are the images when the nanoparticles are pushed, (f) is the amount of voltage change of the piezoelectric ceramic. The nano-friction measured by the experiment and the effective contact area calculated by the simulation are shown in Tab.1 [12].

Tab.1 EXPERIMENT DATA

Radius(nm)	50	100	300
Effective contact area(nm^2)	93.965	188.213	565.204
Nano-friction(nN)	679.626	987.829	2449.816

Tab.2 MAGNIFICATION OF THE MEASURED NANO-FRICTION

Radius(nm)	50	100	300
Friction(nN)	679.63	987.83	2449.82
Magnification	13.86	13.7	13.68

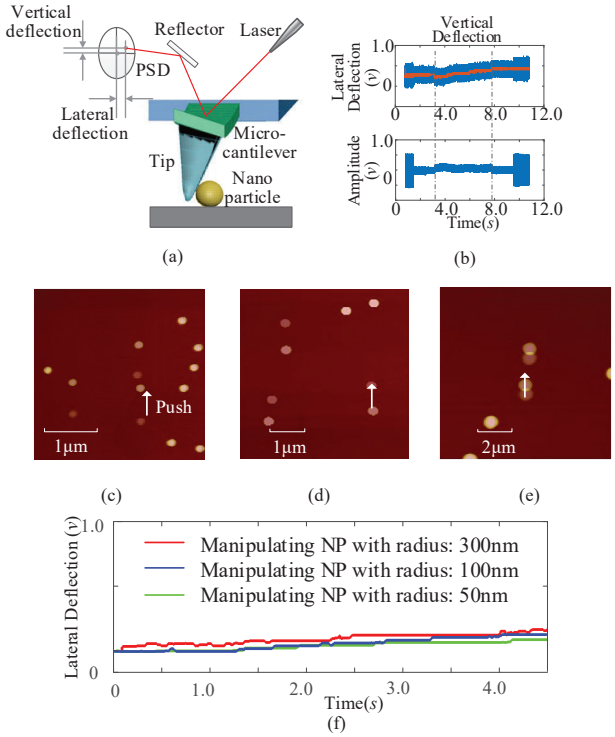

Fig.6 Experimental results

D. Discussion

The relationship between particle radius and nano-friction and the relationship between particle radius and effective contact area are compared with the measured data of nano-friction in reference[13].The result is shown in Fig.7.

Through comparing these curves, it can be found that the nano-friction measured by the experiment is about 13 times larger than the nano-friction in the reference, because $MgCl_2$ solution increase the friction of the surface. It is obvious that the variation tendency of the two results is basically the same. Meanwhile, the nano-friction is in proportion to $R^{2/3}$[14], which illustrates the correctness of the experimental data. The specific magnification is shown in Tab.2.

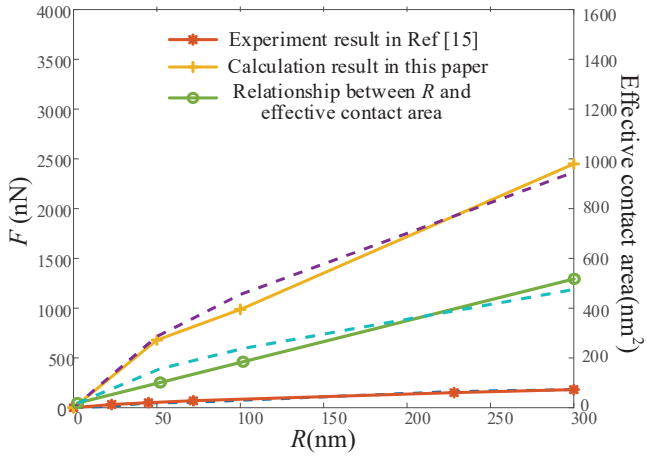

Fig.7 Comparison of nano-friction data and effective contact area

In order to verify the validity of the results, the parameters of the system and carried out a number of simulations are changed. The simulation results are shown in Figure 8. The result shows that the effective contact area A obtained by the simulation satisfies $A \propto R^{4/3}$ under the condition of changing the parameters, which is completely consistent with the previous experiment results by Ritter et al[15]. At the same time, with the increase of particle radius, the influence of particle radius on capillary force will be reduced, and the corresponding friction coefficient will also be reduced, because the conclusion of $F_f \propto R^{2/3}$ has been obtained before, the trend of effective contact area should be faster than that of nano-friction, so follow-up to furtherly prove the correctness of the experimental conclusion. Based on this result, the parameters affecting the effective contact area are analyzed. The result is as shown in Fig.8.

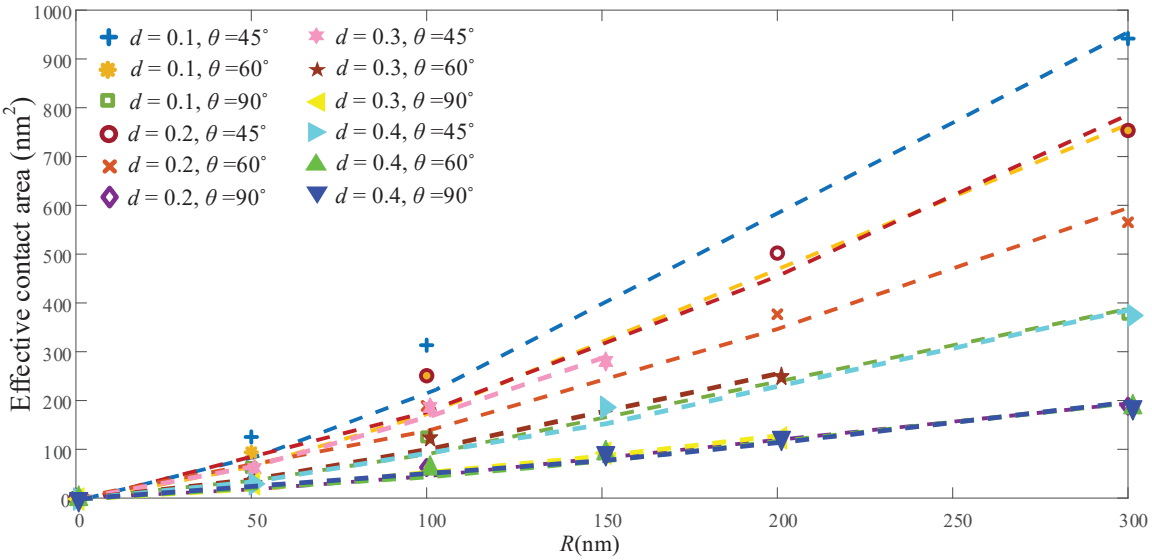

Fig.8 Relationship between effective contact area and R under the condition of different parametersThe Influence of Particle Radius on the Effective Contact Area

1) Relationship between particle radius and effective contact area.

The particle radius will directly determine the effective contact area between the nano-particle and water membrane. In order to more intuitively show the influence of particle radius R and interval distance d on the effective contact area, the relationship between radius R and contact area under the condition of different d was drawn by model. As shown in Fig.9, when the interval distance d is constant, the radius of the nano-particle is directly proportional to the effective contact area.

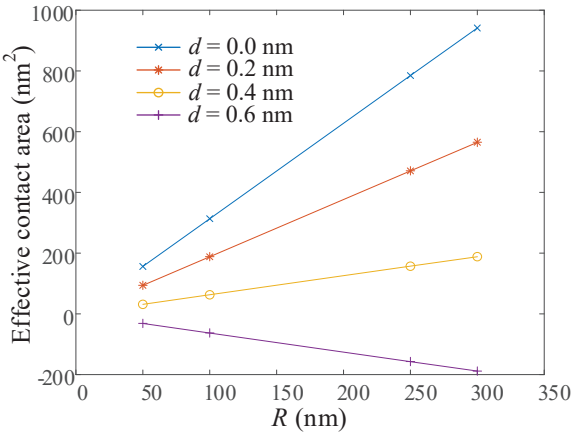

Fig.9 Relationship between particle radius and effective contact area

2) Relationship between interval distance and effective contact area.

In the continuum model, when the distance between the nano-particle and the substrate is 0, a non-zero capillary force can still be predicted even if the relative humidity approaches 0. This is an obviously unrealistic result because there is no water to produce capillary force at all. In practice, there is a minimum limit for $|r_1|$. According to the molecular structure of water, the diameter of a water molecule is about 3 angstroms. If the edge of a meniscus water membrane is composed of one or two water molecules, the curvature cannot be defined under the condition of continuum model and the capillary force will tend to 0. In order to make the continuous model valid, it is necessary to make the interval distance greater than several angstroms, because only in this way can the continuity approximation of the water membrane contour be effective. From another point of view, the calculated capillary force is determined by the contact area of the meniscus water membrane, which depends on the size of the clearance between nano-particle and the substrate that water molecules can fill in.

The relationship between interval distance d and effective contact area under the condition of different particle radius is drawn after simulation in Fig.10. It can be clearly seen that when the radius of the nano-particle is constant, the interval distance d is inversely proportional to the effective contact area.

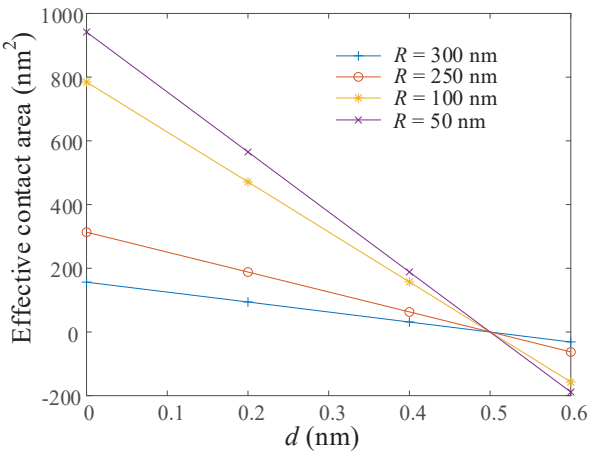

Fig.10 Relationship between interval distance and effective contact area

3) The Influence of Contact Angle on the Effective Contact Area.

Fig.10 shows the water membrane contour when the particle radius is 100 nm and the interval distance is 0.2 nm. The water membrane contour generated when the contact angle is 45°, 60°, 90°, respectively. It can be found that the surface curvature of the meniscus water membrane decreases with the increase of the contact angle. When the contact angle increases, the position of the water membrane contour will change. The larger the contact angle, the smaller the water film contour will be, and the effective contact area will also decrease.

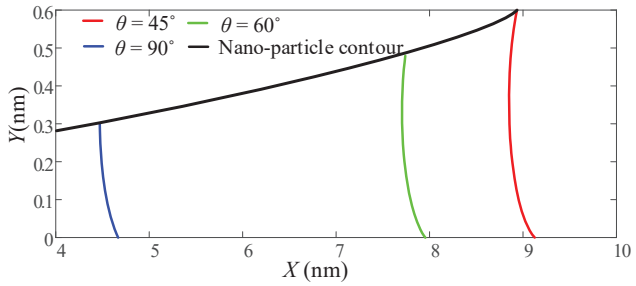

Fig.11 Different meniscus water membrane contour generated by changing contact angle

V. Conclusion

During AFM-based calculation of friction between the nano-particle and the substrate, meniscus water membrane has great influence on measurement result. As for these problems, water membrane model is established and its contour and effective contact area are calculated by using simulation. Meanwhile, the friction is measured by AFM pushing experiment after the tip is positioned by SLAM algorithm. The result is consistent with the existed work. Additionally, the influence of these parameters on the effective contact area of meniscus water membrane is analyzed. These results are of some significance for studying the influence of meniscus water membrane on nano-friction.

References

[1] Gosvami, N.N., J. Ma, and R.W. Carpick, An In Situ Method for Simultaneous Friction Measurements and Imaging of Interfacial Tribochemical Film Growth in Lubricated Contacts. Tribology Letters, 2018. **66**(4): p. 10.

[2] Broitman, E., The nature of the frictional force at the macro-, micro-, and nano-scales. Friction, 2014. **2**(1): p. 40-46.

[3] Chu, E.D., et al., Frictional characteristics of nano-confined water mediated hole-doped single-layer graphene on silica surface. Nanotechnology, 2019. **30**(4): p. 8.

[4] Israelachvili, J.N., Intermolecular and Surface Forces. 3nd. 2011: Academic Press.

[5] Iliev, S.D. and N.C. Pesheva, Dynamic Meniscus Profile Method for determination of the dynamic contact angle in the Wilhelmy geometry. Colloids and Surfaces a-Physicochemical and Engineering Aspects, 2011. **385**(1-3): p. 144-151.

[6] Pakarinen, O.H., et al., Towards an accurate description of the capillary force in nanoparticle-surface interactions. Modelling and Simulation in Materials Science and Engineering, 2005. **13**(7): p. 1175-1186.

[7] Orr, F.M., L.E. Scriven, and A.P. Rivas, Pendular Rings Between Solids - Meniscus Properties And Capillary Force. Journal of Fluid Mechanics, 1975. **67**(FEB25): p. 723-742.

[8] Korayem, M.H., A. Homayooni, and R.N. Hefzabad, Non-classic multiscale modeling of manipulation based on AFM, in aqueous and humid ambient. Surface Science, 2018. **671**: p. 27-35.

[9] Dasgupta, S., et al., Use Of The Augmented Young-Laplace Equation To Model Equilibrium And Evaporating Extended Menisci. Journal of Colloid and Interface Science, 1993. **157**(2): p. 332-342.

[10] Mitropoulos, A., The Kelvin equation. J Colloid Interface Sci, 2008. **317**(2): p. 643-8.

[11] Yuan, S., et al., Stochastic Approach for Feature-Based Tip Localization and Planning in Nanomanipulations. Ieee Transactions on Automation Science and Engineering, 2017. **14**(4): p. 1643-1654.

[12] Bosse, J.L., et al., High speed friction microscopy and nanoscale friction coefficient mapping. Measurement Science and Technology, 2014. **25**(11): p. 9.

[13] Guo, D., et al., Measurement of the Friction between Single Polystyrene Nanospheres and Silicon Surface Using Atomic Force Microscopy. Langmuir, 2013. **29**(23): p. 6920-6925.

[14] Han, J., et al., Tuning the Friction of Silicon Surfaces Using Nanopatterns at the Nanoscale. Coatings, 2018. **8**(1): p. 13.

[15] Ritter, C.; Heyde, M.; Schwarz, U. D.; Rademann, K. Controlled translational manipulation of small latex spheres by dynamic force microscopy. Langmuir 2002, 18 (21), 7798−7803.